Department of Mechanical Engineering
THE UNIVERSITY OF TEXAS AT AUSTIN
Nuclear Engineering Teaching Laboratory • Austin, Texas 78758
512-232-5370 • FAX 512-471-4589 • http://www.me.utexas.edu/~netl/

February 5, 2016

ATTN: Document Control Desk,
U.S. Nuclear Regulatory Commission,
Washington, DC 20555-0001

M. Balazik
Project Manager
Research and Test Reactors Licensing Branch

SUBJECT: Docket No. 50-602, Request for Renewal of Facility Operating License R-129

REF: UNIVERSITY OF TEXAS AT AUSTIN - REQUEST FOR ADDITIONAL INFORMATION REGARDING THE LICENSE RENEWAL REQUEST FOR THE NUCLEAR ENGINEERING TEACHING LABORATORY TRIGA MARK II NUCLEAR RESEARCH REACTOR (TAC NO. ME7694)

Sir:

Analysis has been completed on the two remaining technical issues, including a review of reactivity parameters based on burnup calculations and a loss of coolant accident analysis. An updated validation of reactivity is attached along with a new LOCA thermal hydraulic analysis.

Please contact me by phone at 512-232-5373 or email whaley@mail.utexas.edu if you require additional information or there is a problem with this submittal.

Thank you,

P. M. Whaley
Associate Director
Nuclear Engineering Teaching Laboratory
The University of Texas at Austin

I declare under penalty of perjury that the foregoing is true and correct.
Executed on February 5, 2016

Steven R. Biegalski
NETL Director

A020
NRR

RQUEST FOR ADDITONAL INFORMATION (July 31, 2015: Adams Accession ML15211A362):

The guidance in NUREG-1537 Section 4.5.2, "Reactor Core Physics Parameters," requests the applicant provide calculations of certain core physics parameters and compare them with applicable measurements. A request for additional information was sent to you in a letter dated July 25, 2012 (ADAMS Accession No. ML15211A638), regarding a comparison of calculated and measured values for reactivity parameters. In response, your submittal dated July 15, 2015 (ADAMS Accession No. ML121500308), provided calculations for control rod worth and excess reactivity in Tables 11 and 12, respectively. In addition, you provided comparisons of these\ calculations and measurements in Table 13.

a. In Table 11, your calculations of excess reactivity and control rod worth on 3/16/1992, 7/24/2007, 6/4/2008, 6/11/2008, 6/14/2010, 6/23/2010, 7/25/2011, and 8/2/2012 indicate the shutdown margin for the UT TRIGA reactor would have a positive reactivity. A positive reactivity would not meet Technical Specification 3.2 Shutdown Margin. Please justify why the positive reactivity presents an acceptable level of safety regarding shutdown margin for the UT reactor.

b. In Tables 11 and 12, your calculations for excess reactivity are consistently higher than the measured values. The average bias between the calculated and measured values is $2.56. Please justify why this bias presents an acceptable level of agreement in modeling the UT reactor.

c. Control rod worth in Table 13 appears to be inconsistent. For example, the Regulating Rod worth varies between +12.7% and -21.2%. Specifically, the values for two separate Regulating Rod data points on 7/13/2012, changes from -10.1% to +12.7%. Similarly, Shim-2 worth varies between -23.1% and +30.1%. Please justify why these variations indicate an acceptable level of agreement in modeling the UT reactor.

RESPONSE:

Calibrating model data to measured excess reactivity values indicates all shutdown margins are negative by a wide margin.

Most of the fuel elements in the current UT reactor had been partially burned at other facilities prior to use in this facility. The amount of uranium remaining in an element is based on total core burnup, distributed across the elements in the core. TRIGA peaking factors suggest as much as 40% variation in neutron flux across the core from center to peripheral elements during operation. Investigation of the sensitivity of reactivity calculations to uranium 235 mass indicates a 10% change in mass has on the order of $5 impact on excess reactivity. Given the potential uncertainty in the fuel mass in the partially burned elements, excess reactivity may not be a reasonable function for validating modeling. When reactivity values are adjusted based on calculations assume nominal uranium 235 and 90% of the nominal values and on measured excess reactivity values, integral control rods worth agree to measured values to a reasonable level.

Previous comparisons were based solely on burnup, and did not consider core configurations. As a result, reactivity values for different core configurations were identified by burnup date that did not correspond in all cases to actual core configuration. In considering core configurations and core burnup values, there is general agreement.

ANALYSIS

As previously noted, the initial UT TRIGA core was principally composed of previously (lightly burned) irradiated fuel elements. Special Nuclear Material records were used as a basis for the original uranium composition in material calculations. However, burnup calculations for the Nuclear Materials Management and Safeguards System (NMMSS) track total facility inventory based on core burnup, as opposed to individual fuel elements. Burnup in individual fuel elements varies significantly from average core burnup, and exacerbate potential uncertainty in calculating element-specific burnup.

To evaluate the sensitivity of reactivity values to varying uranium 235 content, calculations were performed for fuel composition using the nominal values from special nuclear material records, and then with 90% of the uranium 235 specifications in the records. The difference between the two values was calculated. The current core contains 114 elements, and additional data is provided for two burn intervals. The deviations in excess reactivity are much higher than the difference in individual integral control rods worth.

Table 1, Reactivity Based on 100% SNM 235 Material Composition and Difference at 90%

		EXCESS	Δ	RR	Δ	SH1	Δ	SH2	Δ	TR	Δ
90	INITIAL	$7.21	-$5.31	$4.33	$0.26	$4.30	-$0.16	$2.53	-$0.03	$2.37	$0.08
	FINAL	$7.09	-$5.18	$4.41	$0.42	$3.94	$0.22	$2.38	$0.39	$2.38	$0.13
89	INITIAL	$8.12	-$5.05	$3.63	$0.56	$3.07	$0.74	$2.66	$0.35	$2.66	$0.26
	FINAL	$7.69	-$5.07	$3.65	$0.46	$2.96	$0.24	$2.61	$0.61	$2.53	$0.14
92	INITIAL	$6.91	-$5.16	$4.55	$0.50	$3.08	$0.90	$2.35	$0.45	$2.05	$0.28
	FINAL	$6.54	-$4.79	$4.07	$0.72	$3.09	$0.69	$2.06	$0.84	$1.67	$0.39
95	INITIAL	$7.44	-$5.09	$4.27	$0.04	$3.16	$0.40	$2.69	$0.21	$2.41	$0.05
	FINAL	$6.32	-$5.36	$4.04	$0.28	$3.18	$0.00	$2.72	-$0.07	$2.24	$0.04
103	INITIAL	$8.04	-$5.69	$3.89	$0.31	$2.98	$0.35	$2.48	$0.20	$2.04	$0.27
	FINAL	$7.71	-$3.59	$4.05	$0.07	$3.24	$0.12	$2.59	-$0.12	$2.19	-$0.06
102	INITIAL	$5.67	-$5.58	$2.69	$0.07	$3.28	$0.33	$2.26	$0.26	$3.21	-$0.08
	FINAL	$4.87	-$4.97	$2.54	$0.81	$2.13	$0.46	$2.43	$0.39	$2.96	$0.30
104	INITIAL	$7.41	-$6.71	$3.32	$0.20	$2.77	$0.30	$3.00	$0.00	$2.76	$0.05
	FINAL	$6.19	-$5.49	$3.43	$0.09	$3.20	-$0.13	$2.86	$0.14	$2.71	$0.06
108	INITIAL	$6.85	-$6.29	$3.09	-$0.22	$2.36	-$0.13	$2.68	-$0.16	$2.63	-$0.25
	FINAL	$6.96	-$5.45	$3.07	$0.42	$2.51	$0.34	$2.98	$0.16	$2.66	-$0.03
110	INITIAL	$6.96	-$5.45	$4.24	-$0.09	$2.35	-$0.07	$3.03	-$0.07	$1.66	-$0.02
	FINAL	$6.89	-$5.08	$3.99	$0.77	$2.91	$0.49	$2.91	$0.49	$1.55	$0.35
114	INITIAL	$4.90	-$3.42	$2.15	$0.38	$2.05	-$0.01	$0.48	$0.55	$0.72	$1.47
114	11.09 MWD	$7.60	-$5.06	$2.61	$0.45	$2.26	$0.48	$2.69	$0.29	$2.74	$0.03
114	35.62 MWD	$7.17	-$5.12	$2.96	$0.45	$2.24	$0.76	$2.70	$0.09	$2.50	$0.12
114	59.88 MWD	$6.91	-$5.18	$2.97	$0.32	$2.65	$0.14	$2.65	$0.14	$2.87	$0.09

Since the excess reactivity (a measured value) appears to be extremely sensitive to uranium 235 content, surveillance data for excess reactivity was used to standardize integral control rod worth values. Integral control rod worth values were linearly interpolated to measured excess reactivity values between the calculated excess and integral control rods worth for 100% and 90% uranium 235 values. Shutdown margin was calculated as excess reactivity less the sum of the integral worth of all control rods. The worth of the most reactive control rod was added to the shutdown margin to simulate the most reactive rod fully withdrawn.

RQUEST FOR ADDITONAL INFORMATION (July 31, 2015: Adams Accession ML15211A362):

The guidance in NUREG-1537 Section 4.5.2, "Reactor Core Physics Parameters," requests the applicant provide calculations of certain core physics parameters and compare them with applicable measurements. A request for additional information was sent to you in a letter dated July 25, 2012 (ADAMS Accession No. ML15211A638), regarding a comparison of calculated and measured values for reactivity parameters. In response, your submittal dated July 15, 2015 (ADAMS Accession No. ML121500308), provided calculations for control rod worth and excess reactivity in Tables 11 and 12, respectively. In addition, you provided comparisons of these\ calculations and measurements in Table 13.

a. In Table 11, your calculations of excess reactivity and control rod worth on 3/16/1992, 7/24/2007, 6/4/2008, 6/11/2008, 6/14/2010, 6/23/2010, 7/25/2011, and 8/2/2012 indicate the shutdown margin for the UT TRIGA reactor would have a positive reactivity. A positive reactivity would not meet Technical Specification 3.2 Shutdown Margin. Please justify why the positive reactivity presents an acceptable level of safety regarding shutdown margin for the UT reactor.

b. In Tables 11 and 12, your calculations for excess reactivity are consistently higher than the measured values. The average bias between the calculated and measured values is $2.56. Please justify why this bias presents an acceptable level of agreement in modeling the UT reactor.

c. Control rod worth in Table 13 appears to be inconsistent. For example, the Regulating Rod worth varies between +12.7% and -21.2%. Specifically, the values for two separate Regulating Rod data points on 7/13/2012, changes from -10.1% to +12.7%. Similarly, Shim-2 worth varies between -23.1% and +30.1%. Please justify why these variations indicate an acceptable level of agreement in modeling the UT reactor.

RESPONSE:

Calibrating model data to measured excess reactivity values indicates all shutdown margins are negative by a wide margin.

Most of the fuel elements in the current UT reactor had been partially burned at other facilities prior to use in this facility. The amount of uranium remaining in an element is based on total core burnup, distributed across the elements in the core. TRIGA peaking factors suggest as much as 40% variation in neutron flux across the core from center to peripheral elements during operation. Investigation of the sensitivity of reactivity calculations to uranium 235 mass indicates a 10% change in mass has on the order of $5 impact on excess reactivity. Given the potential uncertainty in the fuel mass in the partially burned elements, excess reactivity may not be a reasonable function for validating modeling. When reactivity values are adjusted based on calculations assume nominal uranium 235 and 90% of the nominal values and on measured excess reactivity values, integral control rods worth agree to measured values to a reasonable level.

Previous comparisons were based solely on burnup, and did not consider core configurations. As a result, reactivity values for different core configurations were identified by burnup date that did not correspond in all cases to actual core configuration. In considering core configurations and core burnup values, there is general agreement.

ANALYSIS

As previously noted, the initial UT TRIGA core was principally composed of previously (lightly burned) irradiated fuel elements. Special Nuclear Material records were used as a basis for the original uranium composition in material calculations. However, burnup calculations for the Nuclear Materials Management and Safeguards System (NMMSS) track total facility inventory based on core burnup, as opposed to individual fuel elements. Burnup in individual fuel elements varies significantly from average core burnup, and exacerbate potential uncertainty in calculating element-specific burnup.

To evaluate the sensitivity of reactivity values to varying uranium 235 content, calculations were performed for fuel composition using the nominal values from special nuclear material records, and then with 90% of the uranium 235 specifications in the records. The difference between the two values was calculated. The current core contains 114 elements, and additional data is provided for two burn intervals. The deviations in excess reactivity are much higher than the difference in individual integral control rods worth.

Table 1, Reactivity Based on 100% SNM 235 Material Composition and Difference at 90%

		EXCESS	Δ	RR	Δ	SH1	Δ	SH2	Δ	TR	Δ
90	INITIAL	$7.21	-$5.31	$4.33	$0.26	$4.30	-$0.16	$2.53	-$0.03	$2.37	$0.08
	FINAL	$7.09	-$5.18	$4.41	$0.42	$3.94	$0.22	$2.38	$0.39	$2.38	$0.13
89	INITIAL	$8.12	-$5.05	$3.63	$0.56	$3.07	$0.74	$2.66	$0.35	$2.66	$0.26
	FINAL	$7.69	-$5.07	$3.65	$0.46	$2.96	$0.24	$2.61	$0.61	$2.53	$0.14
92	INITIAL	$6.91	-$5.16	$4.55	$0.50	$3.08	$0.90	$2.35	$0.45	$2.05	$0.28
	FINAL	$6.54	-$4.79	$4.07	$0.72	$3.09	$0.69	$2.06	$0.84	$1.67	$0.39
95	INITIAL	$7.44	-$5.09	$4.27	$0.04	$3.16	$0.40	$2.69	$0.21	$2.41	$0.05
	FINAL	$6.32	-$5.36	$4.04	$0.28	$3.18	$0.00	$2.72	-$0.07	$2.24	$0.04
103	INITIAL	$8.04	-$5.69	$3.89	$0.31	$2.98	$0.35	$2.48	$0.20	$2.04	$0.27
	FINAL	$7.71	-$3.59	$4.05	$0.07	$3.24	$0.12	$2.59	-$0.12	$2.19	-$0.06
102	INITIAL	$5.67	-$5.58	$2.69	$0.07	$3.28	$0.33	$2.26	$0.26	$3.21	-$0.08
	FINAL	$4.87	-$4.97	$2.54	$0.81	$2.13	$0.46	$2.43	$0.39	$2.96	$0.30
104	INITIAL	$7.41	-$6.71	$3.32	$0.20	$2.77	$0.30	$3.00	$0.00	$2.76	$0.05
	FINAL	$6.19	-$5.49	$3.43	$0.09	$3.20	-$0.13	$2.86	$0.14	$2.71	$0.06
108	INITIAL	$6.85	-$6.29	$3.09	-$0.22	$2.36	-$0.13	$2.68	-$0.16	$2.63	-$0.25
	FINAL	$6.96	-$5.45	$3.07	$0.42	$2.51	$0.34	$2.98	$0.16	$2.66	-$0.03
110	INITIAL	$6.96	-$5.45	$4.24	-$0.09	$2.35	-$0.07	$3.03	-$0.07	$1.66	-$0.02
	FINAL	$6.89	-$5.08	$3.99	$0.77	$2.91	$0.49	$2.91	$0.49	$1.55	$0.35
114	INITIAL	$4.90	-$3.42	$2.15	$0.38	$2.05	-$0.01	$0.48	$0.55	$0.72	$1.47
114	11.09 MWD	$7.60	-$5.06	$2.61	$0.45	$2.26	$0.48	$2.69	$0.29	$2.74	$0.03
114	35.62 MWD	$7.17	-$5.12	$2.96	$0.45	$2.24	$0.76	$2.70	$0.09	$2.50	$0.12
114	59.88 MWD	$6.91	-$5.18	$2.97	$0.32	$2.65	$0.14	$2.65	$0.14	$2.87	$0.09

Since the excess reactivity (a measured value) appears to be extremely sensitive to uranium 235 content, surveillance data for excess reactivity was used to standardize integral control rod worth values. Integral control rod worth values were linearly interpolated to measured excess reactivity values between the calculated excess and integral control rods worth for 100% and 90% uranium 235 values. Shutdown margin was calculated as excess reactivity less the sum of the integral worth of all control rods. The worth of the most reactive control rod was added to the shutdown margin to simulate the most reactive rod fully withdrawn.

Table 2: Calculated Reactivity Values, Adjusted for Measured Excess Reactivity

		ARO	RR	SH1	SH2	TR	SDM	TS SDM
90	0.00	$5.53	$4.41	$4.25	$2.52	$2.43	-$8.08	-$3.67
	31.07	$5.53	$4.54	$4.01	$2.49	$2.47	-$7.98	-$3.44
89	31.07	$5.53	$3.92	$3.45	$2.83	$3.02	-$7.69	-$3.77
	31.31	$5.50	$3.85	$3.06	$2.87	$2.69	-$6.97	-$3.12
92	31.31	$5.50	$4.69	$3.33	$2.47	$2.21	-$7.20	-$2.51
	36.82	$4.59	$4.37	$3.38	$2.40	$5.16	-$10.72	-$5.56
95	36.82	$4.59	$4.29	$3.39	$2.81	$2.48	-$8.37	-$4.08
	45.72	$5.69	$4.07	$3.18	$2.71	$2.24	-$6.52	-$2.44
103	45.72	$5.69	$4.02	$3.13	$2.56	$2.27	-$6.29	-$2.27
	81.19	$5.77	$4.09	$3.30	$2.53	$2.12	-$6.27	-$2.18
102	81.19	$5.77	$2.69	$3.27	$2.25	$3.22	-$5.66	-$2.39
	106.12	$5.55	$2.43	$2.07	$2.37	$2.84	-$4.16	-$1.32
104	106.12	$5.55	$3.38	$2.85	$3.00	$2.79	-$6.47	-$3.10
	121.82	$5.04	$3.45	$3.17	$2.89	$2.75	-$7.22	-$3.77
108	121.82	$5.04	$3.13	$2.64	$2.79	$2.69	-$6.22	-$3.09
	186.53	$4.45	$3.27	$2.66	$3.06	$2.63	-$7.17	-$3.90
110	186.53	$4.45	$4.20	$2.32	$3.00	$1.64	-$6.71	-$2.51
	204.88	$5.79	$4.16	$3.01	$3.01	$1.66	-$6.06	-$1.90
114-2	226.17	$5.56	$2.79	$2.45	$2.80	$2.78	-$5.27	-$2.47
114-3	226.17	$5.56	$3.10	$2.48	$2.73	$2.60	-$5.35	-$2.25

Control rod worth data is measured periodically to verify that the minimum shutdown margin requirements of Technical Specifications are met. For various reasons the burnup at surveillances does not always correspond well to burnup assumed in analysis (used to determine material compositions for the initiation and termination of core configurations). Previous work did not recognize this difference, comparing only calculated and measured reactivity at the closest applicable burnup.

This effort included ensuring that calculated and measured reactivity values are compared for similar burnup values and core configurations. Data indicates the model is consistent with operating data. The comparison of calculated to measured reactivity data (Table 3) is calculated as:

$$D = \frac{\delta k_M - \delta k_C}{\delta k_M}$$

Where D is the deviation from measured values, δk_M is the reactivity from measured data, and δk_M is the reactivity based on the model.

Table 3, Comparison Measured and Calculated Data

SURVIELANCE		CALCULATION		REACTIVITY COMPARISON					
DATE	MWD	CORE	MWD	RR	SH1	SH2	TR	ROD SUM	SDM
07/01/92	0.00	90i	0.00	-8.02%	-40.28%	20.55%	25.37%	-0.51%	-1.37%
04/27/00	31.31	90f	31.07	-0.80%	-15.16%	8.67%	-4.72%	-3.35%	-5.81%
		89i	31.07	12.95%	0.96%	-3.81%	-27.96%	-1.13%	-1.96%
		89f	31.31	14.34%	12.11%	-5.08%	-13.91%	4.59%	7.56%
		92i	31.31	-4.17%	4.31%	9.62%	6.31%	2.86%	4.56%
07/30/01	45.81	95f	45.72	2.76%	1.77%	7.92%	6.87%	4.47%	20.41%
		103i	45.72	4.13%	3.51%	12.86%	5.68%	6.28%	23.22%
11/14/02	81.29	103f	81.19	4.93%	1.12%	8.16%	15.56%	6.70%	13.10%
		104i	106.12	-1.36%	-2.59%	7.63%	16.08%	5.25%	6.45%
07/18/05	121.93	104f	121.82	-12.45%	-7.85%	7.95%	16.27%	1.37%	-4.93%
07/25/07	186.65	108f	186.53	-14.98%	3.19%	7.36%	20.68%	4.85%	0.02%
06/29/10	226.30	114_1	215.97	3.77%	3.36%	9.95%	11.46%	7.39%	10.75%
		114_2	240.50	-6.82%	2.24%	12.31%	17.26%	6.71%	9.39%

LOSS OF COOLANT ACCIDENT ANALYSIS FOR THE UNIVERSITY OF TEXAS AT AUSTIN TRIGA REACTOR

1. Introduction

The loss of coolant accident (LOCA) analysis assumes steady state reactor operation at equilibrium (limiting core configuration conditions) followed by a reactor scram with the water cooling simultaneously replaced with air cooling. The analysis models radial heat transfer from the center of the element outward to the air at the axial location/segment of the hot channel fuel element with the maximum specific power.

This LOCA analysis includes (1) an overview of the analysis, (2) specific characteristics of UT TRIGA system, (3) the basis of thermodynamic analysis, (4) development of the UT finite element analysis model, (5) validation of the model against independent analytical method and against measured data, and (6) analysis of the thermodynamic characteristics following a LOCA with initial conditions established by the limiting core configuration.

2. UT TRIGA Characteristics

Heat generation following shutdown is a product of decay heat from fission products generated during operation, and has the same spatial distribution as power generation during operation. Analysis requires calculation of decay heat as a function of time. Thermodynamic properties of TRIGA fuel are taken from reference material. A set of derived thermodynamic properties (i.e., dimensionless numbers) is calculated. The decay heat, fuel geometry, and derived thermodynamic properties are incorporated in model to simulate time dependent thermal dynamic response loss of water coolant.

2.1. Decay Heat

Calculations with TRACE indicate the maximum power for a fuel element with an acceptable critical heat flux ratio of 2.0 is slightly less than 24 kW; the assumed initial condition for the maximum power in a fuel element is therefore 23 kW. Neutronic analysis with the fuel element divided into 15 equal axial segments shows the maximum power generation in a single axial segment is 1.2 times the average segment or 1.84 kW for the initial conditions of the power generation in the maximum segment of the "hot channel." The decay heat is simulated as a heat source within the fuel element geometry.
The decay power fraction remaining after an abrupt shutdown is found by equation[1]:

$$R(t) = \frac{0.04856 + 0.1189 \cdot \log_{10} t - 0.103 \cdot (\log_{10} t)^2 + 0.000228 \cdot (\log_{10} t)^3}{1 + 2.5481 \cdot \log_{10} t - 0.19632 \cdot (\log_{10} t)^2 + 0.05417 \cdot (\log_{10} t)^3} \quad (1)$$

The fuel temperature of the element producing the maximum power level in the core (hot channel) is the most severe condition for heat transfer from the core during operation. For the limiting case, the maximum specific power and the decay power fraction in the fuel element is calculated from the maximum axial peaking factor for the fuel element:

$$q_{gen,i}(t,r) = 1.2 \cdot q_{gen}(r) \cdot R(t) \quad (2$$

[1] Kansas State, "Kansas State University Safety and Analysis Report '06." KSU, Manhatten, 2006.

The radial distribution of power in each element remains constant, while the magnitude decreases with time after shutdown according to eqn. (1).

2.2. Fuel Element Geometry

The fuel element model in this analysis is a set of concentric cylinders representing a zirconium rod at the center, the fuel matrix, a gas-gap between the fuel and cladding, and cladding. The dimensions are taken from the GA drawings and UT Technical Specifications. The Zirconium fill rod diameter is 0.25 in (0.6125 cm) in diameter. The fuel matrix outer diameter is 1.47 in (3.6015 cm) diameter. The gas gap is approximately 0.005 in (1.97E-3 cm). Cladding is 0.020 in (0.0489 cm) thick. The total heated length of the fuel (section with Zr-U fuel matrix) is 15 in, segmented for thermal hydraulic analysis into 15 equal lengths. In this analysis only the vertical segment with the highest heat generation rate is considered.

2.3. Fuel Element Thermodynamic properties

Simnad[2] provides a number of mechanical characteristics and equations for fuel quantities. The thermal conductivity (k) is given, density is calculated from a given equation for a specific Zr:H ratio of 1.6. Density is based off of an equation for the 8.5 wt% U:

$$\rho_{Fuel} = \frac{1}{\left(\frac{U_{wt\%}}{\rho_U}\right) + \frac{(1 - U_{wt\%})}{\rho_{Zr}}} \tag{3}$$

Where $U_{tw\%}$ is uranium weight per cent, ρ_U is the density of uranium, and ρ_U is the density of zirconium. Simnad provides the temperature (T) dependent volumetric heat capacity ($c_{p,vol}$):

$$c_{p,vol}\left\{\frac{J}{m^3 K}\right\} = 2.04 + 4.17e - 3 \cdot T \tag{4a}$$

Specific heat capacity ($c_{p,fuel}$) is calculated as the ratio of eqn. (4) to eqn. (3).

$$c_{p,fuel}\left\{\frac{J}{kg * K}\right\} = \frac{\rho_{Fuel}}{c_{p,vol}} \tag{4b}$$

3. Basis of Thermodynamic Analysis

The general thermodynamic basis in this analysis is based on an energy balance:

$$\dot{E}_{st} = \dot{E}_{gen} + \dot{E}_{in} - \dot{E}_{out} \tag{5a}$$

[2] M. T. Simnad, "The U-ZrHx Alloy: Its Properties and Use in TRIGA Fuel," *Nucl. Eng. Des.*, vol. 64, pp. 403–422, 1981.

Where, $\dot{E}_{st}$ is the stored energy in the structure, $\dot{E}_{gen}$ is energy generated within the structure, $\dot{E}_{in}$ is energy transferred into the structure, and $\dot{E}_{out}$ is the energy transferred out of the structure. This model translates into:

$$\rho \cdot V \cdot c_p \cdot \frac{dT}{dt} = q_{gen} + q_{cond} + q_{conv} \tag{5b}$$

Stored energy (and the associated temperature change) is a function of material density (ρ), specific heat (c_p), volume (V), and the conduction, convection, and generation terms (q_{gen}, q_{cond}, and q_{conv} respectively).

3.1 Stored Energy ($\rho \cdot V \cdot c_p \cdot T$)

Energy storage is related to material properties and temperature, an important factor in calculating the temperature transient analysis.

3.2 Energy Generation (q_{gen})

Energy generation in the core is a result of fission inside the element.

3.4 Conduction Heat Transfer (q_{cond})

Heat transfer through conduction within the radius of the fuel element and cladding is modelled with Fourier's law of conduction using radial geometry:

$$q_{cond} = -k \cdot A_s \cdot \frac{dT}{dr} \tag{6}$$

Where k is thermal conductivity, A_s is the surface area through which heat transfer occurs, and $\frac{dT}{dr}$ is the rate of temperature change with respect to radial displacement. As recommended by Fenech[3], the gas gap is approximated as thermal conductivity, calculated by the gas gap coefficient divided by the radial thickness of the gap.

3.5 Convection Heat Transfer (q_{conv})

Convection applies to the surface element where heat is transferred from the fuel element to the surrounding air. Convection heat transfer is modelled using Newton's law of cooling:

$$q_{conv} = h \cdot A_s \cdot (T_s - T_{inf}) \tag{7}$$

Where the wall surface area is A_s, the wall temperature is T_s, and the bulk coolant temperature is T_{inf}, and the heat transfer coefficient is h. The convection heat transfer coefficient is calculated from dimensionless numbers. For natural convection, the significant dimensionless numbers are the Prandtl (Pr), Grashof (Gr), and modified

[3] H. Fenech, "Heat Transfer and Fluid Flow in Nuclear Systems," Pergamon Press (1981)

Rayleigh (Ra) numbers. These values, combined with Nusselt (Nu) correlations, lead to the heat transfer coefficients which are used to find the energy transferred via convection.

a. The Prandtl number is a measure of the fluid's kinematic diffusivity (ν) to thermal diffusivity (α) of the fluid:

$$Pr = \frac{\nu}{\alpha} \tag{8}$$

Where thermal diffusivity of the fluid is calculated as:

$$\alpha = \frac{k}{c_p \cdot \rho} \tag{9}$$

(6)

b. The Grashof number (and implicitly, values derived from the Grashof number) are dependent on both surface temperature and channel temperature. The Grashof number (for natural circulation heat transfer) is defined as:

$$Gr_s = \frac{g \cdot \beta \cdot (T_s - T_{inf}) \cdot s^3}{\mu^2} \tag{10}$$

Where g is the acceleration due to gravity, β is the thermal expansion coefficient of the coolant, s is the channel width, and μ is the dynamic viscosity of the coolant.

c. The Rayleigh number is calculated [Kaminski[4]],:

$$Ra_s = Gr_s Pr = \frac{g\beta\rho^2(T_{wall} - T_{fluid})s^3}{\mu^2} Pr \tag{11}$$

Where s is the total channel width.

d. The Nusselt number relates the conductive and convective heat transfer effects of the fluid. The heat transfer is driven by the temperature difference and is found through the Nusselt number. A correlation for natural circulation in vertical channels for the Nusselt number[4] is:

$$Nu_s = \left\{ \frac{576}{\left[Ra_s\left(\frac{s}{dy}\right)\right]^2} + \frac{2.87}{\left[Ra_s\left(\frac{s}{dy}\right)\right]^{1/2}} \right\}^{-1/2} \tag{12}$$

e. The average heat transfer coefficient, $\bar{h}$, can be found from the average Nusselt number using[5]:

[4] D. A. Kaminski, , M. K. Jensen, "Introduction to Thermal and Fluids Engineering," John Wiley & Sons (2005)

$$\bar{h} = \frac{\overline{Nu}_s.k}{s} \tag{13}$$

4 The UT LOCA Model

The University of Texas Loss of Coolant model is a combination of finite element analysis (FEA) for steady state, and transient fuel conditions, as well as an air channel analysis sub-section to provide effective estimation of air channel heating. This channel sub-model leads to proper parametric variation analysis by giving a real world upper bounding temperature.

4.1 Coolant Air Temperature

In order to find the limiting values of the channel air temperature, a separate, one dimensional vertical model was created independent of the FEA model and geometry used in finding the fuel temperatures. It utilizes an elemental, vertical, constant temperature surface interfacing with buoyant air.

The temperature entering the bottom of the channel surrounding the fuel element is the limiting room air temperature following a loss of coolant, 20°C. The rise in temperature is found by segmenting the pin vertically. Each iteration has a specific heat flux relative to the temperature difference between the surface and the air, its specific dimensionless parameters, and a constant surface temperature that is user defined. The limiting conditions set the surface temperature at 950C. This was the value used later as a limiting factor in FEA parametric variation.

The change in air temperature across each segment is a function of the heat generated in the segment and the heat transfer coefficient calculated from local non-dimensional parameters. Heat transfer characteristics in convection depend on intrinsic and extrinsic material properties and fluid temperature, with the heat transfer coefficient calculable though the use of dimensionless numbers. The temperature rise of the fluid entering the region of heat transfer for subsequent segments is the exit temperature for the preceding segment, i.e., the rise in temperature across the previous segment added to the temperature of the coolant entering the previous segment. The channel flow heat up model provided an order of magnitude estimation leading to proper parametric variation.

4.1.1

Fluid flow, and thus the characteristic velocity, is driven by natural convection and is dominated by the buoyancy driven numbers in the Rayleigh number (Ra_s), the product of the Grashof and Prandtl numbers.

a. The change in coolant temperature from fluid flow across a segment begins by finding the appropriate Rayleigh number (eqn. 11) for the i^{th} segment [Kaminski[6]],

---

[5] T. L. Bergman, A. S. Lavine, F. P. Incropera, and D. P. DeWitt op cit & C. O. Popiel and J. Wojtkowiak, "Simple formulas for thermophysical properties of liquid water for heat transfer calculations (from 0 to 150 degrees C) (vol 19, pg 87, 1998)," Heat Transf. Eng., vol. 19, no. 3, pp. 87–101, 1998.

[6] D. A. Kaminski, , M. K. Jensen, "Introduction to Thermal and Fluids Engineering," John Wiley & Sons (2005)

then the segment's Nusselt number (eqn. 12), then the heat transfer coefficient (eqn. 13). With the heat transfer coefficient now found, the heat flux (q'') is found using:

$$q'' = h_i \cdot (T_s - T_{inf,i}) \tag{15}$$

Where T_s is the cladding surface temperature and $T_{inf,i}$ is the heat sink temperature.

b. Heat flux is used to find the Modified Rayleigh number. For uniform wall heating, the modified Rayleigh $(Ra^*)^3$ is:

$$Ra_s^* = \frac{g \cdot \beta \cdot q'' \cdot \rho^2 \cdot c_p \cdot s^4}{\mu \cdot k^2} \tag{16}$$

Where g is the acceleration due to gravity, β is the thermal expansion coefficient, and μ is dynamic viscosity.

c. The modified Rayleigh number leads to the characteristic channel velocity[7] (U_Z):

$$U_z = \frac{\alpha}{s}\sqrt{Ra_L^* \cdot Pr} \tag{17}$$

d. The change in temperature for fluid flow across a segment of the fuel element along the (axial) direction of flow can be calculated with:

$$\dot{Q}_i = \dot{m} \cdot c_p \cdot \Delta T \tag{18}$$

e. Where the ΔT is calculated as:

$$\Delta T = \frac{q'' \cdot A_{FE,i}}{\rho \cdot A_{flow} \cdot U_Z \cdot c_p} \tag{19}$$

Where U_Z is calculated from eqn. (19). This ΔT is added to the segment's inlet temperature and becomes the inlet temperature for the next segment. The last segment's channel temperature represents the culmination of all the heating.

4.1.2 As an independent calculation to determine limiting values of air temperature, the temperature rise was found through standard gas laws.

a. The characteristic velocity gives a stay time for the air (heated length divided by characteristic channel velocity). This allows the change in energy to be calculated as follows:

$$dE = q'' \cdot A_s \cdot t_{stay} \tag{20}$$

[7] K. Vafai, C. P. Desai, S. V. Iyer, and M. P. Dyko, "Buoyancy Induced Convection in a Narrow Open-Ended Annulus," *J. Heat Transfer*, vol. 119, p. 483, 1997.

Where t_{stay} is the time the cooling air is in contact with the cladding surface.

b. By using the density of air and the volume of the channel, the mass of the air in the space at any given time can be found, by neglecting density changes. Using the equation below, the change in temperature can be found:

$$q = mc_v\Delta T \rightarrow \quad (21)$$
$$\Delta T = \frac{q}{mc_v} \Rightarrow T_f = T_{init} + \Delta T$$

4.1.3 Results of calculations for limiting values of the channel air temperature

These two methods routinely agreed across variations in surface temperatures, with the limiting channel temperature, of 20°C inlet and 950°C surface temperature, being 35.3°C.

4.2 Finite Element Model Geometry and Basis

The calculation of temperature distribution in the fuel element is accomplished by using the principles of finite element analysis. The fuel element geometry is based on a cylindrical segment. The axial height of the segment is the total heated length (0.381 m) divided by the number of segments (15). Radial dimensions are taken from General Atomics drawings.

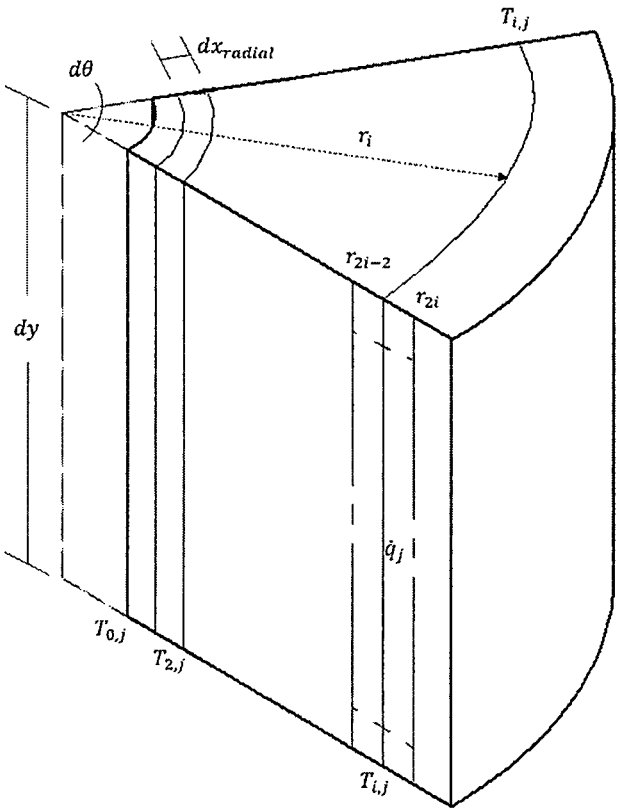

Figure 1. Finite Element Radial Geometry

The Finite Element Model radii used in computation was selected based on both parameter validation and computational power available. The limiting geometric figure of concern is the Biot number, which relates convective and conductive aspects of the element to its volume to surface area ratio. It is determined using the equation below:

$$Bi = \frac{h \cdot L_c}{k} \tag{22a}$$

Where, the characteristic length, L_c, is defined as the volume to surface area ratio:

$$L_c = \frac{V}{A} \tag{22b}$$

Differential radii in the outer portions of the model were chosen to most accurately subdivide the real geometry of the cladding and the gas gap. Internal fuel differential radii were chosen to minimize the Biot number. In addition to the Biot number, the Fourier number is a transient figure of merit related to constants that determine time response and the geometry:

$$Fo = \frac{\alpha \cdot t}{L_c} \tag{23}$$

According to Bergman[4], the Biot number must remain below 0.1, and the Fourier number must remain below 0.5 for lumped parameter analysis to be valid. This was the merit to which the differential radii are chosen.

4.3 Steady State Finite Element Analysis

To create a valid transient condition, a valid steady state initial condition must be found. To facilitate this, each element is assessed using an energy balance equation across the element. Since the steady state model is not time dependent, the energy balance is reduced to:

$$\dot{E}_{in} + \dot{E}_{gen} = \dot{E}_{out};\ \dot{E}_{out} = 0 \implies \dot{E}_{in} + \dot{E}_{gen} = 0 \tag{24}$$

In this analysis, energy flow is considered into the element. Fig. 2 illustrates element energy balance and temperature relationship.

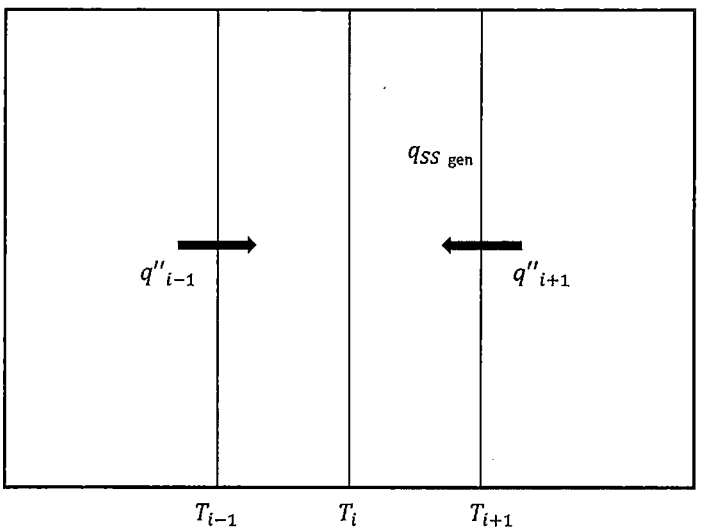

Figure 2. Finite Element Energy Balance

A matrix form of this energy balance is developed to solve for the temperature profile.

$$A\vec{x} = \vec{b} \tag{25}$$

Where, $\vec{x}$ is a vector representing the radial temperature profile, and $\vec{b}$ is a vector representing the energy generation and non-temperature dependent terms. Below is the development of the steady state finite element equations. The cladding end element is the only element containing a convection term, while fuel elements are the only ones containing generation terms. The following relationships are incorporated in the elements of the matrix equations:

Conduction and Convection Terms:

$$q_{gen,SS,r} = q_{max} \cdot q(r) \cdot \pi \cdot dy \cdot ({r_{2i}}^2 - {r_{2i-2}}^2) \tag{26a}$$

$$q_{conv,SS} = h_{water} \cdot \pi \cdot r_{max} \cdot dy \cdot (T_s - T_{inf}) \tag{26b}$$

$$q_{cond,SS} = \frac{2 \cdot \pi \cdot dy \cdot k_{fuel} \cdot (T_{i\pm1} - T_i)}{\ln\left(\frac{r_{larger}}{r_{smaller}}\right)} \tag{26c}$$

Generation and Temperature Independent Terms

$$b_i = -q_{max} \cdot \pi \cdot dy \cdot ({r_{2i}}^2 - {r_{2i-2}}^2); \tag{26d}$$

$$b_{end-1,4} = 0; \ \ (No\ heat\ generation\ in\ cladding/gas) \tag{26e}$$

$$b_{end} = -h_{water} \cdot \pi \cdot r_{end} \cdot dy \cdot T_{inf} \tag{26f}$$

Matrix Elements for $\boldsymbol{A} = \begin{bmatrix} a_1 \\ a_2 \\ \vdots \\ a_j \\ a_{end} \end{bmatrix}$

$$a_1 = \left[\frac{2 \cdot \pi \cdot dy \cdot k_{fuel} \cdot (T_{i-1} - T_i)}{\ln\left(\frac{r_2}{r_1}\right)}, \quad \frac{-2 \cdot \pi \cdot dy \cdot k_{fuel} \cdot (T_{i+1} - T_i)}{\ln\left(\frac{r_2}{r_1}\right)} \ \ldots \right] \tag{26g}$$

(26h)

$$a_i = \left[\ldots, \frac{2 \cdot \pi \cdot dy \cdot k_{fuel(gas,clad)} \cdot (T_{i-1} - T_i)}{\ln\left(\frac{r_{2i-1}}{r_{2i-3}}\right)}, -\left(\frac{2 \cdot \pi \cdot dy \cdot k_{fuel(gas,clad)} \cdot (T_{i-1} - T_i)}{\ln\left(\frac{r_{2i-1}}{r_{2i-3}}\right)} + \frac{2 \cdot \pi \cdot dy \cdot k_{fuel(gas,clad)} \cdot (T_{i+1} - T_i)}{\ln\left(\frac{r_{2i+1}}{r_{2i-1}}\right)} \right), \frac{2 \cdot \pi \cdot dy \cdot k_{fuel(gas,clad)} \cdot (T_{i+1} - T_i)}{\ln\left(\frac{r_{2i+1}}{r_{2i-1}}\right)} \ \ldots \right]$$

(26i)

$$a_{end} = \left[\ldots, \frac{2 \cdot \pi \cdot dy \cdot k_{clad} \cdot (T_{end-1} - T_{end})}{\ln\left(\frac{r_{end}}{r_{end-1}}\right)}, \right.$$
$$\left. -\left(\frac{2 \cdot \pi \cdot dy \cdot k_{clad} \cdot (T_{end-1} - T_{end})}{\ln\left(\frac{r_{end}}{r_{end-1}}\right)} + h_{water} \cdot \pi \cdot r_{end} \cdot dy \right) \right]$$

Matrix Formula

$$\vec{T} = \boldsymbol{A}^{-1} \cdot \vec{\boldsymbol{b}} \tag{26k}$$

The energy generation term in the element is a function of both its axial and radial position. The highest axial peaking factor (1.2) was used to represent the cylindrical segment generating the most power. The radial peaking factor, q(r), is found through a curve fit to neutronic code output, with the highest axial peaking factor of 1.2.

MATLAB was utilized to build and solve the equation using native commands that maximize the efficiency and accuracy of the matrix inversion method.

4.4 Transient Finite Element Analysis

Heat transfer analysis for systems that have time variation can be analyzed using lumped parameter analysis where the internal resistance to heat transfer is small compared to convection resistance, and the characteristic time constants are similarly related. The transient portion of the model takes the initial steady state temperature profile and systematically walks it forward with time. The basic concept of an energy balance as used in the steady state analysis is maintained, with the time dependent components now considered in addition to the other terms. In the UT LOCA model the loss of coolant accident is considered to be instantaneous, and thus the cooling properties switch from water to air.

$$\dot{E}_{st} = \dot{E}_{in} - \dot{E}_{out} + \dot{E}_{gen};\ \dot{E}_{out} = 0 \rightarrow \tag{27a}$$

$$\rho \forall c_p \frac{dT}{dt} = q_{cond} + q_{conv} + q_{gen} \rightarrow \tag{27b}$$

$$\rho \forall c_p \frac{(T_i^{p+1} - T_i^p)}{\Delta t} = q_{cond} + q_{conv} + q_{gen} \tag{27c}$$

This leads to the transient analysis equation set which is related to the steady state equations as follows:

$$T_i^{p+1} = \frac{\Delta t}{\rho \forall c_p}[a_i] + T_i^p \tag{28}$$

The differential time element is selected based on the merit of the Fourier number previously mentioned. Additionally, the code calculates a number of output values including a two-dimensional matrix $\vec{B}$ whose horizontal dimension represents the radial temperature

distribution and whose vertical axis represents time. This allows three essential model parameters to be extracted. First, the cladding surface temperature versus time is extracted and used to find peak cladding temperature. Second, the temperature profile across the pin at t_i can be found. Third, the maximum temperature both radially and through time can be found.

5 Model Validation

5.1 Comparison of TRACE and the UT MATLAB model Steady State Temperature Profile

The core configuration contains 114 fuel elements, with a core radial peaking factor derived from SCALE physics calculation for the core (prior to January 2016) of 1.6, and a maximum axial peaking factor of 1.2. The current normal operating power is 950 kW. The power generated in the maximum segment of the hot channel for comparison using data prior to January 2016 is therefore 12.5 kW.

The steady state solution using water coolant was developed for the maximum power level in a fuel element operating at 12.5 kW and compared to the TRACE calculations (Fig. 3). The TRACE and FEA calculations are in substantial agreement with experimental data.

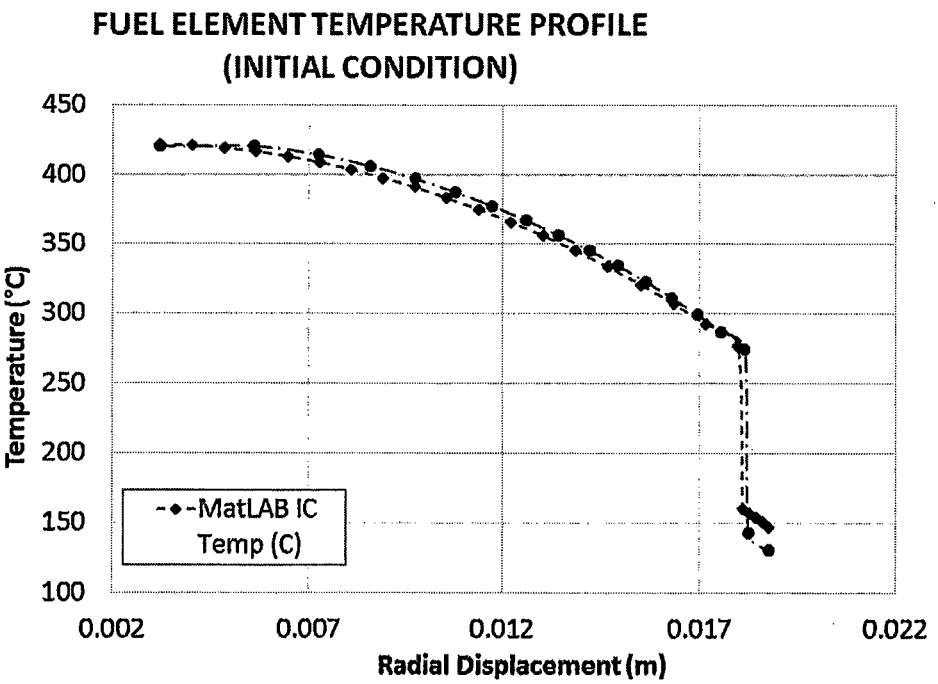

Figure 3. TRACE and UT LOCA model steady state temperature profiles

5.2 Comparison of FT2 Observations and Calculations (TRACE, UT MATLAB Model) Steady State Temperature Response to Power Operation

The MATLAB finite element analysis was applied at power generation in an element from 200 W to the 12.5 kW, and the maximum element temperature compared to the TRACE and FT2 measurements (taken prior to January 2016) across the range.

TRACE and the MATLAB based steady state temperature calculations in radial locations associated with thermocouples are essential the same. There is good agreement between calculated and observed values with some deviation at higher power levels where the heat transfer is presumably affected by the development of bubbles that enhance heat transfer and reduce fuel temperature (Fig. 4).

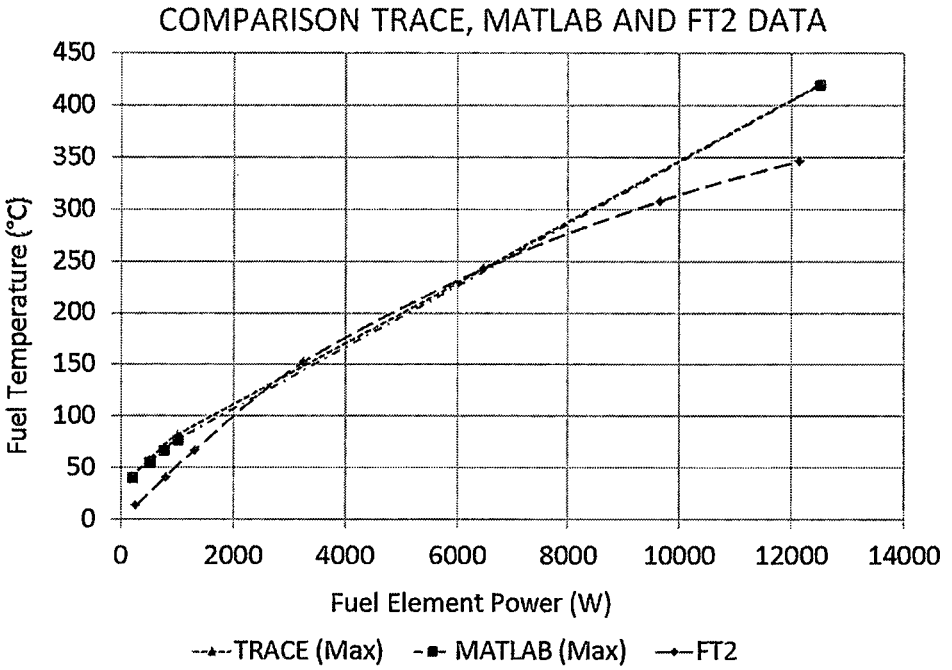

Figure 4. Comparison of Temperatures from Calculations and Observations at Varying Power Levels

5.3 Comparison of FT2 Observations and Calculations (TRACE, UT MATLAB Model) Transient Temperature Response to Shutdown from Normal Operations

Transient fuel temperature was observed following a shutdown from power operations at 950 kW (Fig. 5, FT2 Data). Calculations were performed to simulate the transient using TRACE (Fig. 5, TRACE Calc) and MATLAB based model (Fig. 5, UT MATLAB). The temperature data is in good agreement.

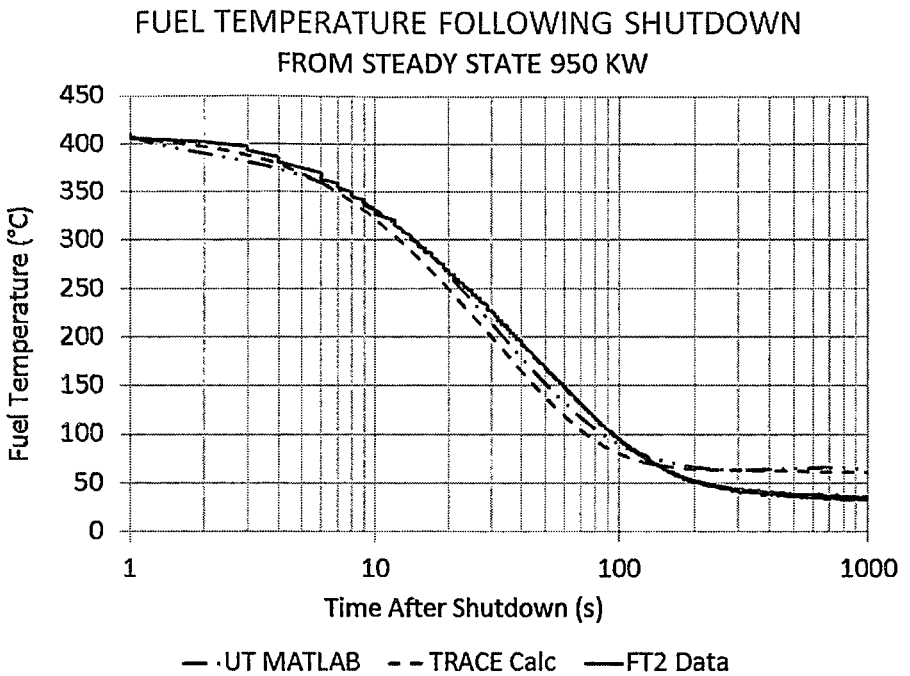

Figure 5. Fuel Temperature, Measuring Channel & Calculations Following Reactor Scram

5.4 Summary

Comparison of fuel temperature measuring channel data to calculated fuel temperatures during steady state and transient conditions is in good agreement. The agreement between observations and calculations during steady state operations suggests the method is fundamentally correct. The agreement between observations and calculations during transient operations suggests the method will provide reasonably accurate time-dependent calculations.

6 Results

The UT MATLAB model calculation was performed for various values of both air channel temperature and pin power. The radial temperature profile of the fuel element segment generating the highest power in the core is provided in Fig. 6 following a shutdown from normal full power operation at 950 kW operations with air cooling at inlet air temperature equal to UT rector bay nominal temperature.

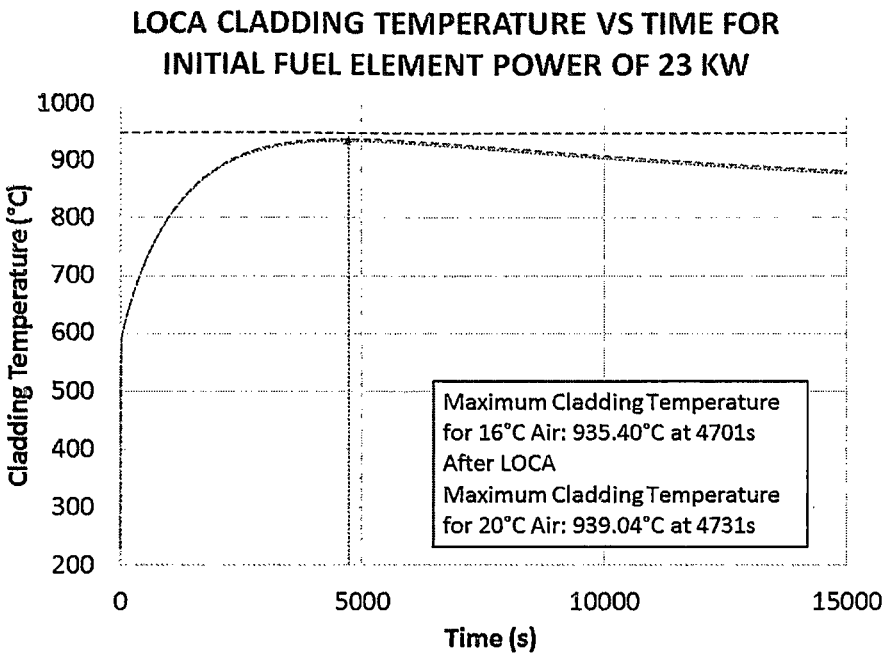

Figure 6. LOCA Cladding Temperature vs Time

Fuel element power level and inlet air temperature were varied to provide an indication to sensitivity to the parameters (Fig. 7). Line labels used in or significant to this analysis are provided with label markers.

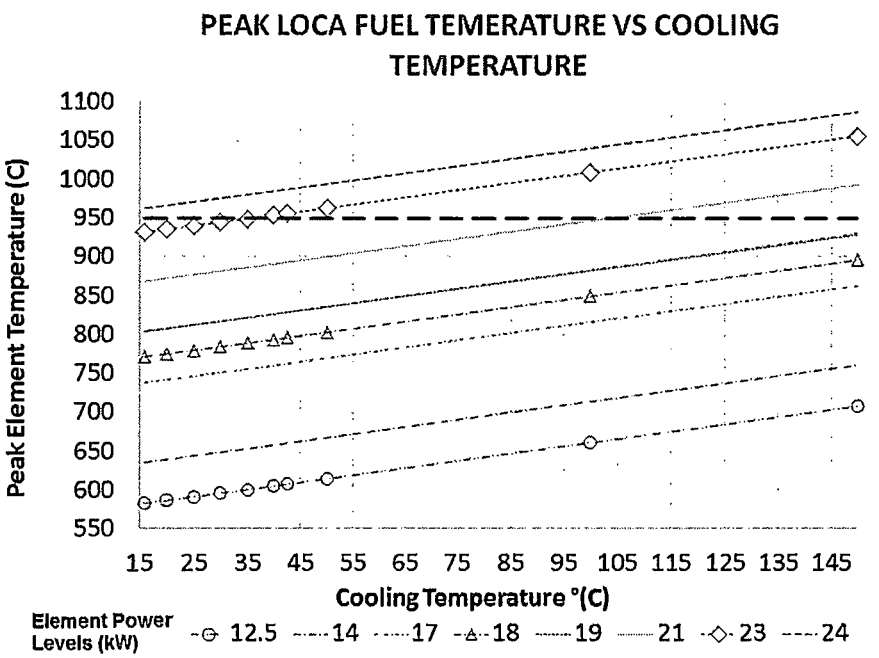

Figure 7. Peak Fuel Temperature during Loss of Coolant Accident

For reactor bay air at 16°C, the maximum fuel element power prior to LOCA initiation that could achieve 950°C fuel temperature with air cooling is 23.6 kW. At 23 kW generated in the fuel element during operation prior to the LOCA initiation (the maximum power generated in a fuel

element in the limiting core configuration), air inlet temperature inlet less than 35°C is calculated not to exceed 950°C fuel temperature. Therefore a LOCA following normal steady operation with a fuel element operating at 23 kW will not exceed the fuel temperature safety limit.

This analysis is extremely conservative in several important respects, including neglecting axial conduction, assuming an instantaneous loss of cooling water, assuming a complete loss of water, and assuming dry air.

a. The UT LOCA model takes place at the point of highest axial power production and only transmits energy radially, while in reality the axial conduction effects would work to reduce the maximum fuel temperature prior to and during the transient.

b. As shown in Fig. 5, water cooling immediately following shutdown reduces fuel temperature significantly, with the measuring channel indicating 100°C decrease over about 13 seconds. A smaller quantity of stored heat reduces fuel temperature at the initiation of the LOCA.

c. The most probable flow path for a LOCA is via failure in beam port casing. The beam ports are located slightly below core center, and a substantial fraction of the core structure and fuel elements will be in contact with pool water even if drained to the bottom of the beam ports.

d. The specific heat capacity of dry air is 1 kJ/kg-K, but the reactor bay ventilation system is designed to control relative humidity for comfort. Specific heat capacity for moist air is calculated[8]:

$$c_v = 1.005 + (8 \cdot 10^{-7} \cdot T^2 + 2.5 \cdot 10^{-7} \cdot T + 1.86) \cdot H$$

The specific heat capacity of moist air increases with relative humidity, so that calculations with dry air result in lower heat transfer and higher fuel temperatures. In addition, the nature of the event assures moist air in the cooling supply.

[8] http://www.engineeringtoolbox.com/